

Ventilation Design Considerations for Occupant Health in Aircraft Painting Facilities Under OSHA Requirements

James S. Bennett, PhD

Member ASHRAE

ABSTRACT

Reducing exposures of aircraft painters to hazardous metals and organics motivates design and operation of hangar ventilation systems in purpose-built facilities. Facilities are often repurposed for aircraft painting, even when the ventilation system has been designed for thermal comfort or general dilution. Contaminant exposures under cross-flow, ceiling diffuser, and hybrid ventilation configurations were evaluated. Occupational Safety and Health Administration (OSHA) regulations require 100 fpm (0.508 m/s) through spray booths/rooms, and this condition is difficult to achieve with most ceiling diffuser installations. Cross-flow designs provided lower contaminant exposures, with decreased residence times and efficient flow paths. CFD modeling, tracer gas testing, and exposure monitoring examined contaminant exposure vs. crossflow ventilation velocity. RANS CFD modeling (RNG $k-\epsilon$) showed exposures to simulated methyl isobutyl ketone of 294 and 83.6 ppm, as a spatial average of five worker locations, for velocities of 0.508 and 0.381 m/s (100 and 75 fpm), respectively. In tracer gas experiments, observed supply/exhaust velocities of 0.706/0.503 m/s (136/99 fpm) were termed full-flow, and reduced velocities were termed 3/4-flow and half-flow. Half-flow showed higher tracer gas concentrations than 3/4-flow, which had the lowest time-averaged concentration, with difference in log means significant at the 95% confidence level. Half-flow compared to full-flow and 3/4-flow compared to full-flow showed no statistically significant difference. CFD modeling using these ventilation conditions agreed closely with the tracer results for the full-flow and 3/4-flow comparison, yet not for the 3/4-flow and half-flow comparison. Full-flow conditions at the painting facility produced a velocity of 0.528 m/s (104 fpm) midway between supply and exhaust locations, with the supply rate of 94.4 m³/s (200,000 cfm) exceeding the exhaust rate of 68.7 m³/s (146,000 cfm). Ventilation modifications to correct this imbalance created a midhangar velocity of 0.406 m/s (80.0 fpm). Personal exposure monitoring for two worker groups—sprayers and sprayer helpers (“hosemen”)—compared process duration means for the two velocities. Hexavalent chromium (Cr[VI]) exposures were 500 vs. 360 µg/m³ for sprayers and 120 vs. 170 µg/m³ for hosemen, for 0.528 m/s (104 fpm) and 0.406 m/s (80.0 fpm), respectively. Hexamethylene diisocyanate (HDI) monomer means were 32.2 vs. 13.3 µg/m³ for sprayers and 3.99 vs. 8.42 µg/m³ for hosemen. Crossflow velocities affected exposures inconsistently, and local work zone velocities were much lower. Aircraft painting contaminant control is accomplished better with the unidirectional crossflow ventilation presented here than with other observed configurations. Exposure limit exceedances for this ideal condition reinforce continued use of personal protective equipment.

INTRODUCTION

National Institute for Occupational Safety and Health (NIOSH) researchers investigated ventilation system performance in military aircraft paint finishing hangars as a function of air velocity delivered by the system to the work area. Previous investigations at the subject facility found exposures to isocyanates and hexavalent chromium exceeded occupational exposure limits (OELs) (Bennett et al. 2016). Isocyanates are respiratory sensitizers and have health effects in both monomeric and oligomeric forms (U.S. DHHS 1996, 2006; Vandenplas et al. 1993; Bello et al.

2004). Hexavalent chromium exposure can cause nasal irritation and damage, and respiratory cancer, among other conditions (U.S. DHHS 2015).

OSHA standard, 29 CFR 1910.94 – *Ventilation*, requires that spray booths maintain an air velocity in the booth cross-section of 100 fpm (0.508 m/s) (Code of Federal Regulations). However, an OSHA interpretation of 1910.94 prepared for the subject facility stated that its hangar is a spray area rather than a booth. Evaluating ventilation performance, then, should perhaps focus more on exposure control than velocity achievement, although 100 fpm (0.508 m/s) is still required by the 2010 Uniform Facilities Criteria (UFC) (U.S. DoD 2010). The hexavalent chromium (Cr[VI]) standard, 29 CFR 1910.1026, part (f)(1)(ii), on painting large aircraft, allows respiratory protection to achieve the PEL (5 $\mu\text{g}/\text{m}^3$), if 8-hr TWA concentrations controlled through other methods do not exceed 25 $\mu\text{g Cr[VI]}/\text{m}^3$, “unless the employer can demonstrate that such controls are not feasible” (Code of Federal Regulations). Because respirators reduce rather than eliminate exposure, work area concentration remains important. Interestingly, the ACGIH recommends only 50 fpm (0.254 m/s) for large vehicle paint booths (ACGIH 2010).

The subject facility was designed to meet the 100 fpm (0.508 m/s) velocity specification; however, separate bays of the facility consistently operated at velocities that differed from the specification. The bays were geometrically identical, including the ventilation configuration, and the air handling equipment for each bay was of the same brand and model number. Operational differences were attributed to controller settings, wear, and filter loading. These facts allowed investigation of velocity as an exposure determinant.

Motivation for the investigation came from exceedances of OELs when the ventilation system met the OSHA and UFC criterion of 5.08 m/s (100 fpm). A question followed naturally—is this velocity the most protective? Understanding the effect of velocity (within a reasonable range) on exposure then became the study focus, with the large effect of velocity on energy use a secondary consideration.

METHODS

The supply and exhaust filter banks in these bays were smaller than the cross-sectional area of the hangar. All air velocities (V_{cs}) reported here were normalized to the area of the hangar cross-section (A_{cs}), using the formula

$$V_{cs} = (A/A_{cs}) V \quad (1)$$

where A and V are the face area and face velocity of the supply or exhaust filter banks. This approach was used to facilitate comparison with regulations and guidance for spray operations ventilation, which are given as velocities in the occupied cross-section, rather than as volumetric flow rates. The supply and exhaust filter areas were 86.6% and 37.5% of the cross-sectional area, respectively (Figure 1).

Comprehensive air sampling evaluating concentrations of compounds in paints, primers, and solvents used on F/A-18C/D Hornet strike fighter aircraft was reported previously (Bennett et al. 2016). The current study includes follow-up sampling of total particulate matter (TPM), hexavalent chromium Cr[VI], and hexamethylene diisocyanate (HDI) after ventilation system modifications. The exposures were normalized by comparing the six observations from the original survey to the single observation in the follow-up survey, treated as a reference value, and a percent-difference was calculated, forming $N = 6 \times 4 = 24$ comparisons by velocity. Statistical analysis showed that the personal exposure data were log-normally distributed, and a t-test was performed on the log-transformed data. Additional details are available in Bennett, Marlow, Nourian, et al. (2018).

CFD Methods. The steady-state, differential form of the incompressible Navier-Stokes equations, along with the transport equations for turbulence quantities and species mass, were discretized to the computational grid, using the SIMPLE algorithm and the second-order upwind discretization scheme. Simulations were performed for a variety of ventilation settings representing both balanced and unbalanced flow rates. Aircraft surfaces and hangar wall, floor, and ceiling were modeled as no-slip walls, except that for the unbalanced flow conditions, the ceiling was modeled as a zero-gauge pressure boundary. A user-defined contaminant with the density and viscosity of methyl isobutyl ketone

(MIBK) was emitted at a volumetric flow rate specified by the spray gun manufacturer, in vapor form, from the hand areas of two simulated workers placed at commonly observed spraying locations. Once dispersed, the fluid properties were determined by the volume fractions of contaminant and clean air in the hangar air mixture, according to the species concentration determined by the coupled solution process, wherein flow, turbulence, and concentration variables are updated in each iteration. A 9.5 million cell unstructured mesh composed of both tetrahedral and hexahedral elements, of an F/A-18C/D Hornet centered in the hangar space, was generated. The extent of the computational domain matched the interior of the hangar bay depicted in Figures 1 and 2. The modeled geometry included positions of wing flaps, elevators, and rudders, observed during painting. Hosemen (H) were placed farther from the aircraft and downwind from their sprayer (S) partners. The contaminant source was located at the end of the sprayers' right arms. One sprayer was on a scaffold. Solutions were initialized by applying supply filter boundary conditions—velocity, TI (10%), L (1 m), and MIBK concentration (zero)—to all fluid cells, then brought to iterative convergence, where the normalized residuals were all less than 10^{-3} , using the first order upwind discretization scheme (Patankar 1980). All simulations were then run for 38,000 iterations, using second order upwind discretization, where the normalized residuals were below 10^{-4} , except in the case of species (less than 10^{-5}) and eddy dissipation rate (slightly greater than 10^{-4}). Concentration never clearly asymptoted but achieved regular fluctuations within a limited range. The fixed and large number of iterations was used as the ultimate convergence requirement to ensure exposure comparisons among flow conditions suffered only small and similar convergence errors.

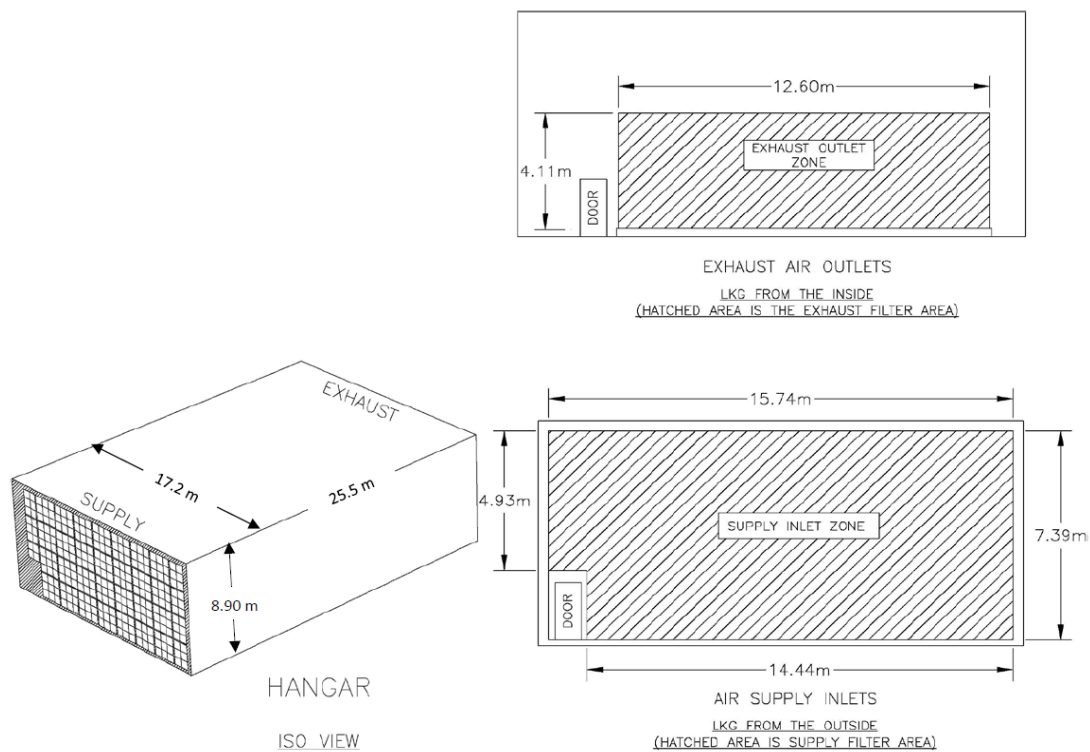


Figure 1. Drawing of the aircraft painting bay showing filter areas.

Tracer Experiments. Sulfurhexafluoride (SF_6) was released in the unoccupied hangar—with the F-18 aircraft in place—at the normal supply/exhaust flow rate and at lower flow rates, and concentrations were measured at various locations. The concentrations of SF_6 were compared among three unbalanced flow rates—half, 3/4, and full capacity determined by the number of supply blowers operating—with the exhaust attempting to match these rates

and falling short, in each case. Thus, the experiments were conducted with this system operating normally, and with one of four supply-exhaust pairs powered down and also with two supply-exhaust pairs down. SF₆ was released continuously at the aircraft nose and measured at five observed worker locations, using portable real-time infrared monitors. Several 15-minute trials were run, in a randomized factorial design, with “ventilation setting” as the independent variable and time-averaged SF₆ concentration the dependent variable (U.S. DHHS 2012). A multiple comparison analysis (Tukey’s studentized range test) on the log mean concentrations, with velocity scenario as a categorical variable, used the 95%-confidence level.

Completing the Concentration Curve. After developing an understanding of the effect on worker exposure of three crossflow ventilation velocities, CFD was used to look at additional velocities toward developing a concentration and velocity relation for this painting operation. The same CFD methods were used in these simulations as in the previous work, but convergence was handled differently. For these analyses, the simulated relation was compared to the classical expectation that the product CQ is a constant value, as is strictly true for complete and instantaneous mixing and for well-developed dynamic dilution.

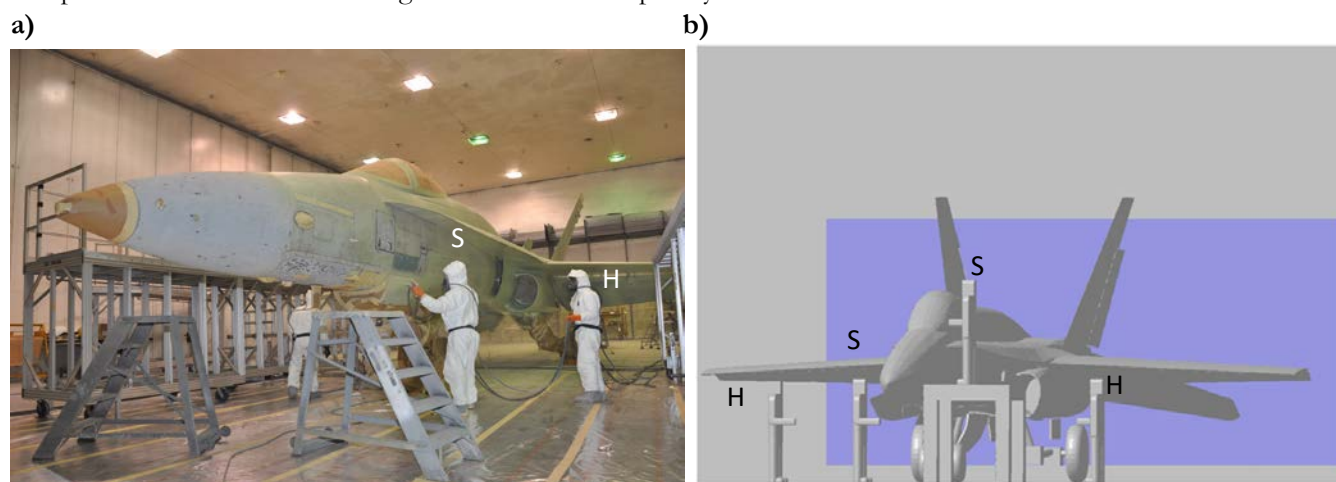


Figure 2. a) Navy artisans (sprayers and hosemen) applying primer during F-18 strike fighter aircraft paint finishing operations. b) Geometry of workers, exhaust wall filter, and F/A-18C/D Aircraft.

RESULTS

Air Velocities. In the initial survey, the supply rate of 94.4 m³/s (200,000 cfm) produced an average velocity of 0.798 m/s (157 fpm) at the supply filter face. The supply velocity normalized to the hangar cross-section was 0.691 m/s (136 fpm), which exceeded the original design specification of 0.508 m/s (100 fpm). The exhaust rate of 68.7 m³/s (146,000 cfm) produced an average velocity of 1.34 m/s (264 fpm) at the exhaust filter face, which normalized to 0.504 m/s (99.3 fpm). As shown in Table III, these supply and exhaust conditions created a measured velocity of 0.528 m/s (104 fpm) in the mid-hangar work zone. In the follow-up survey, the average mid-hangar velocities were 0.412 m/s (81.1 fpm) for the large bay created by combining Bays 7 and 8 and 0.406 m/s (80.0 fpm) for Bay 2.

Aircraft Primer Paint Spraying. TPM process duration TWAs for sprayers in the current survey was 14 mg/m³ compared to 18 mg/m³ in the initial survey, and TPM for hosemen in the current survey was 5.9 mg/m³ compared to 4.3 mg/m³ in the initial survey. The single-measurements, for sprayers and hosemen in the current survey, fell within the initial survey data range, for each job classification.

The Cr[VI] result for sprayers in the current survey was 360 µg/m³ compared to 500 µg/m³ in the initial surveys. The Cr[VI] result for hosemen in the current survey was 170 µg/m³ compared to 120 µg/m³ in the initial survey. The single-value at the lower velocity of the current survey, when compared to the initial survey, was lower for sprayers and higher for hosemen, while remaining within the data range for each job classification.

Aircraft Topcoat Painting. HDI monomer geometric means, comparing results for all three aircraft in the follow-up survey to the initial survey (F-18 only), were 13.3 $\mu\text{g}/\text{m}^3$ vs. 32.2 $\mu\text{g}/\text{m}^3$ for sprayers and 8.42 $\mu\text{g}/\text{m}^3$ vs. 3.99 $\mu\text{g}/\text{m}^3$ for hosemen, while oligomer concentrations (as NCO) were 310 $\mu\text{g}/\text{m}^3$ vs. 259 $\mu\text{g}/\text{m}^3$ for sprayers and 192 $\mu\text{g}/\text{m}^3$ vs. 42.7 $\mu\text{g}/\text{m}^3$ for hosemen. Although the work task of painting C-2, E-2, or F-18 aircraft was observed to be essentially the same, differences in coating composition and aircraft geometry introduce some variability. Looking only within the F-18 data, then, HDI monomer results were 30.9 $\mu\text{g}/\text{m}^3$ vs. 32.2 $\mu\text{g}/\text{m}^3$ for sprayers and 19.6 $\mu\text{g}/\text{m}^3$ vs. 3.99 $\mu\text{g}/\text{m}^3$ for hosemen, while oligomer concentrations (as NCO) were 725 $\mu\text{g}/\text{m}^3$ vs. 259 $\mu\text{g}/\text{m}^3$ for sprayers and 673 $\mu\text{g}/\text{m}^3$ vs. 42.7 $\mu\text{g}/\text{m}^3$ for hosemen.

Statistical Comparisons. Table IV compares exposures according to bay ventilation velocity. Bay velocity had a statistically significant effect for hosemen, and the negative mean difference indicates that lower velocity led to higher exposure. This result is consistent with the dynamic dilution concept, and conservation of mass requires that within some zone in the ventilated space, higher velocity will create lower concentration. The effect was not seen for sprayers, where the mean difference comparing higher velocity exposures to lower velocity exposures was positive, while not statistically significant. It is possible that the lower velocity was weakly protective for sprayers, but a reasonable interpretation is that it had no discernable effect. When the t-test was done on the mean differences with hosemen and sprayers combined (N reduced to 8), significance disappeared, as the 95% confidence interval included zero.

CFD Modeling. Figure 3a shows concentration contours in the vertical plane bisecting the bay and the aircraft. The shapes of the plumes from the two sprayers (on the scaffold and under the wing) indicate that the crossflow ventilation system provided reasonably directional flow through the work zone, even with the spray momentum and eddy diffusion creating the circular pattern near the sprayers. Figure 3b shows that CFD simulations at 0.381 m/s (75 fpm) produced lower concentrations than 0.508 m/s (100 fpm), at the highest concentration locations.

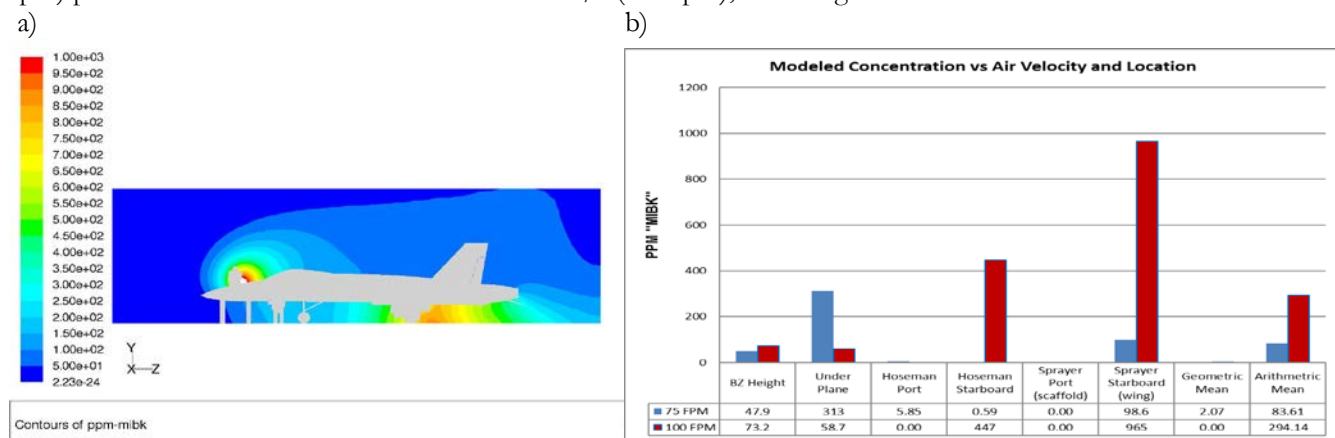


Figure 3. a) Modeled MIBK contours (ppm) on bay centerplane, showing sprayer on the scaffold, hoseman standing on the ground, and the plume created by the sprayer underneath the far wing. b) CFD results at 0.381 m/s (75 fpm) and 0.508 m/s (100 fpm). “BZ Height” refers to the entire hangar, at a height of 1.50 m from the floor. The heights of “Under Plane,” “Hoseman Port,” “Hoseman Starboard,” “Sprayer Port (scaffold),” and “Sprayer Starboard (wing),” were 0.305 m, 1.50 m, 1.50 m, 3.00 m, and 1.50 m, respectively.

Verification and Validation. The grid of 9,476,802 cells was adapted to a fine grid of 16,241,731 cells (a 42% increase). Local velocities and TKEs for the original and the finer grid were identical to three significant figures. Sufficient grid resolution in the boundary layer around the F-18 surfaces and the workers are indicated by first-cell y+ values all being less than one. Figure 4a shows CFD and tracer experiment concentration means across monitoring locations. To compare the predicted effects of velocity, CFD concentrations were divided by tracer gas concentration at full-flow to create a normalized reference value. Both methods showed a similar decrease in concentration when the flow was lowered from full- to 3/4-flow. Tracer experiments indicated a large increase in normalized

concentration when the velocity was decreased further, from 3/4- to half-flow. In the CFD simulations, however, there appears to be no discernable difference between concentrations at 3/4- and half-flows.

Thus, the CFD techniques employed here were consistent with the tracer gas results in the moderate and high ventilation velocity range and inconsistent in the low velocity range. This latter behavior, unfortunately, is commonly seen, and the remedy is computationally expensive. The k-ε turbulence models may underestimate the effect that velocity fluctuations have on contaminant transport (Lin et al. 2005). Because velocities varied across the real filter faces, whereas the simulation boundary conditions were uniform, it is possible that the simulations created a more effective velocity field for contaminant removal, with fewer flow reversals. Figure 4b shows the effect of flow reduction through multiple pair-wise comparisons. Tracer location means, in blue, along with their 95% error bars for Tukey's studentized range HSD test, are plotted with the CFD results. Half-flow concentrations being statistically significantly higher than 3/4-flow is shown here by the confidence interval staying above zero. For the 3/4 vs. full comparison, CFD and tracer results diverge. Interestingly, all CFD predictions are at or within the 95% confidence limits for the tracer measurements.

Tracer Gas Experiments. Recall that the supply/exhaust velocities in the tracer gas experiments were: full-flow, 0.706/0.503 m/s (139/99.0 fpm); 3/4-flow, 0.518/0.350 m/s (102/68.9 fpm); and, half-flow, 0.371/0.249 m/s (73.4/49.0 fpm). As shown in Figure 4b, SF₆ concentrations at the five monitoring locations were higher for half-flow than for 3/4-flow, with statistical significance (95% confidence intervals did not include zero). No statistically significant difference was found between half-flow and full-flow or 3/4-flow and full-flow. The rate of 3/4-flow had the lowest mean concentration. This unbalanced rate created a measured hangar midpoint velocity of 0.374 m/s (73.6 fpm), whereas the half-flow and full-flow conditions produced velocities of 0.365 m/s (71.8 fpm) and 0.528 m/s (104 fpm) respectively. The closeness of the midpoint velocities for 3/4- and half-flows should not be interpreted as precisely representing the velocities through the work area, since the 16-point measurement matrix was somewhat coarse for the hangar bay crosssectional area of 134 m². The velocity fields were probably better represented by considering the measured supply, midpoint, and exhaust velocities together.

Completing the Concentration Curve. Figure 5a plots the simulation results along with $C = k/V$ curves for comparison with the classical expectation. The breathing zone concentration drops quickly with increasing velocity, until what looks roughly like 70 fpm, above which there seems to not be much exposure control gained. The $C = k/V$ curve based on the simulated concentration at 25 fpm shows much less control efficiency. However, Figure 5b shows that the steep power law decrease of concentration continues up to 100 fpm (0.508 m/s).

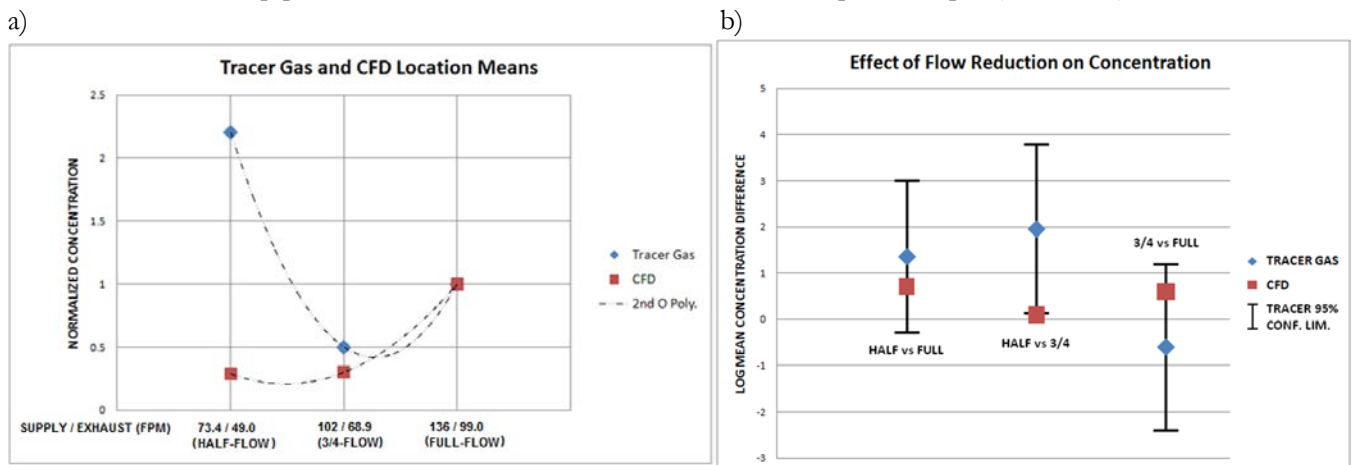


Figure 4. a) Five-location-mean concentrations for CFD simulations and tracer gas experiment means, as a function of velocity. b) Flow rate comparison by CFD and tracer gas methods.

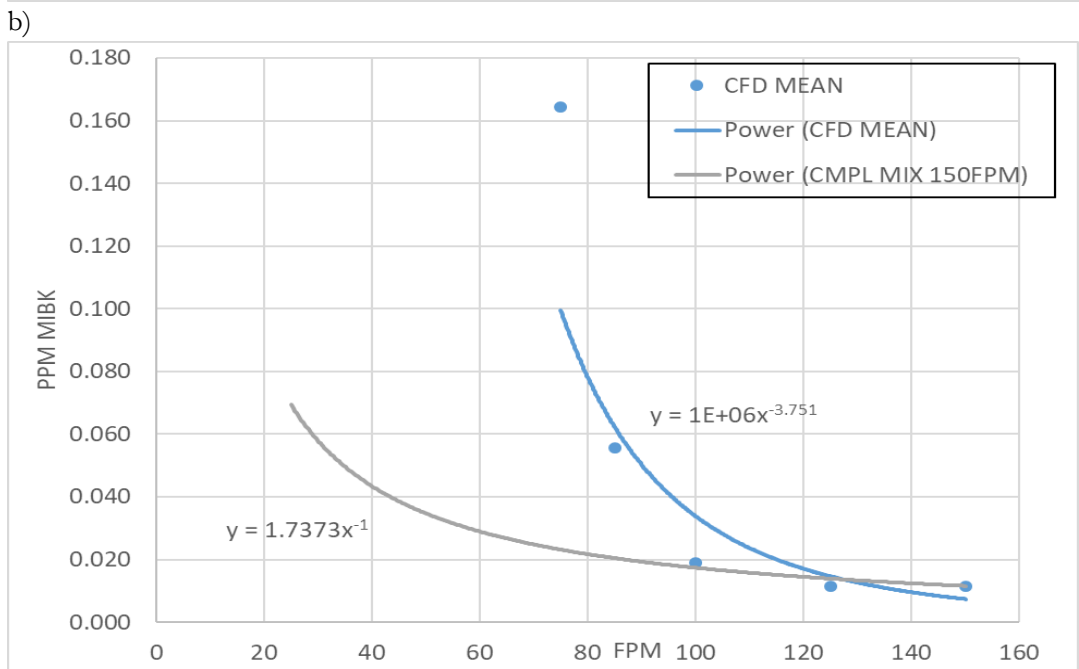
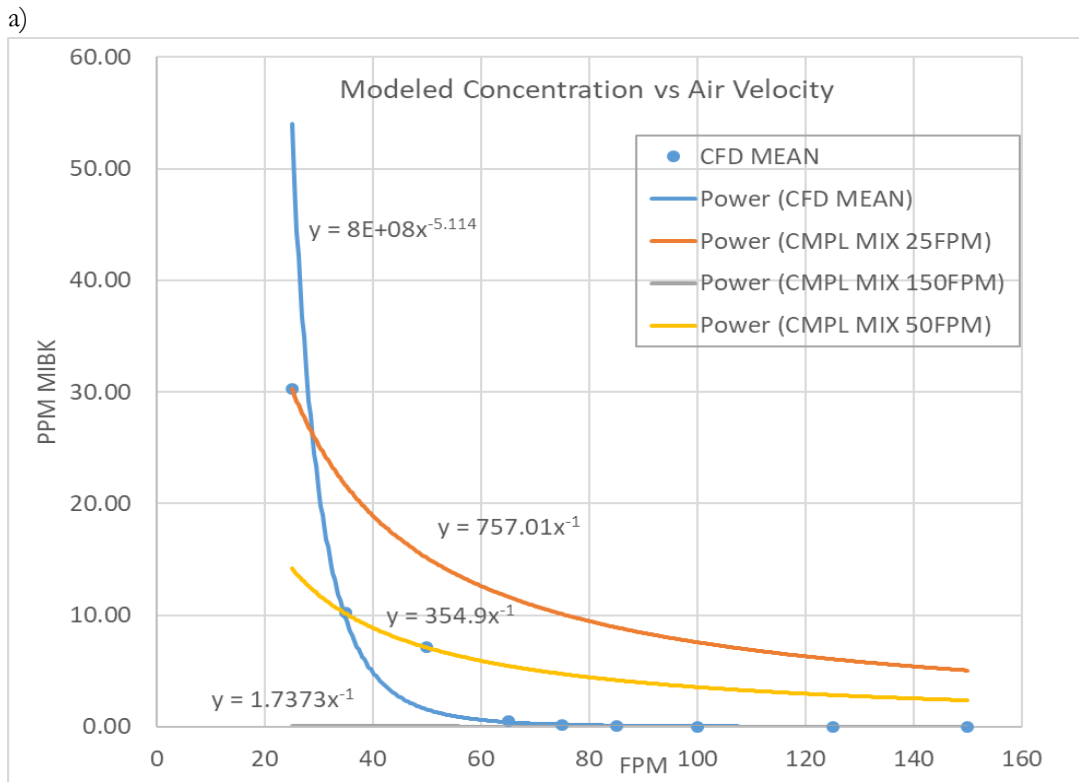


Figure 5. (a) CFD concentration behavior over the range 25 to 150 fpm (0.127 to 0.762 m/s), compared to completely mixed (CM) models based on CFD concentrations at 25, 50, and 150 fpm. CM curves are V^{-1} power law and the CFD data fit curve is approximately V^{-5} . (b) Detail of concentration at higher velocities, showing CFD concentration data follows the CM curve only at 100 fpm and above.

DISCUSSION

The isocyanate, hexavalent chromium and total particulate results that compared the initial and follow-up surveys did not show a consistent relationship between ventilation velocity and contaminant concentration. CFD simulations and tracer experiments both indicated a substantial increase in worker protection when the ventilation velocity was increased from the low range, 0.254 – 0.335 m/s (50 – 66 fpm), to either the moderate range, 0.381 – 0.406 m/s (75 – 80 fpm), or the high range, 0.432 – 0.528 m/s (85 – 104 fpm). The tracer and CFD simulations of the tracer experiment conditions indicated that the range 0.254 to 0.335 m/s (50 to 66 fpm) was clearly too low, and a physical interpretation is that the flow was subject to meandering. A reasonably unidirectional flow path should be the goal in crossflow ventilation. CFD simulations comparing 0.381 and 0.508 m/s (75 and 100 fpm) showed 75 fpm to be more protective (Figure 4), whereas Figure 5b shows the exposure to drop when velocity was increased from 75 to 85 and then to 100 fpm. Figure 5a puts this solution region into perspective, as something that might be considered noise. The three sets of CFD simulations gave varying concentration results in this range of velocity. Differences in solution convergence, averaging of the concentration results over the final iterations, and instability in the concentration values near “zero,” as the air parcel concentration in the breathing zone switched from a value less than the machine tolerance ($\sim 10^{-35}$) to a clearly non-zero value. Care was taken within each set of CFD simulations to strictly adhere to a solution extraction protocol.

Mixing is not efficient exposure control. Examining now Figures 5a and b, the crossflow ventilation performance is far more efficient than complete mixing (CM), as the concentration drop with additional velocity is approximately a fifth-order phenomena, whereas CM behavior is a first-order drop. Figures 5a and b show three velocity regions: very rapid concentration drop with velocity from 25 to 65 fpm, more gradual decrease that remains more effective than CM from 65 to 100 fpm, and then essentially CM from 100 to 150 fpm. In terms of the CM formula, these phenomena can be written:

$$C_{CFD} \ll k_1[G_{CFD}/Q_{CFD}], 25 \leq V < 65 \text{ fpm} \quad (2);$$
$$C_{CFD} < k_2[G_{CFD}/Q_{CFD}], 65 \leq V < 100 \text{ fpm} \quad (3); \quad C_{CFD} \approx k_3[G_{CFD}/Q_{CFD}], 100 \leq V \leq 150 \text{ fpm} \quad (4).$$

CONCLUSION

Crossflow ventilation velocity of approximately 0.254 m/s (50 fpm) was less effective at exposure reduction than either 0.381 or 0.508 m/s (75 or 100 fpm). No general difference was clearly discernable between 0.381 and 0.508 m/s (75 and 100 fpm), although local exposures did vary with velocity. That a maintained linear rate of approximately 0.508 m/s (100 fpm) provided inadequate protection creates a caution against over-reliance on the intuitive concept that more ventilation is better. Moreover, because velocity increases lead to exponentially increased energy use, while possibly adding no protective value, flow paths that provide efficient unidirectional contaminant removal should be foundational in aircraft painting ventilation design. It appears there are, for the scenario studied, lower velocity domains where the ventilation control of exposure to the painters is more efficient than $C = k/V$ and higher velocity domains where it is approximately the same as $C = k/V$. Pairing this observation with the exposure monitoring and tracer results, and giving some consideration to the strong (cubic) dependence of energy consumption on velocity, suggests an operating point for crossflow ventilation in this operation of approximately 75 fpm. If the most important performance criterion is reducing exposure as much as possible, despite vanishing benefit, then the top velocity available and within other strictures such as comfort, physical safety, and paint application might be indicated.

NOMENCLATURE

A	=	Area	C	=	Air contaminant concentration
G	=	Contaminant generation rate	k_i	=	Arbitrary constants
Q	=	Volumetric flow rate	V	=	Velocity

REFERENCES

- American Conference of Governmental Industrial Hygienists (ACGIH): *Industrial Ventilation—A Manual of Recommended Practice*, 27th Edition. Cincinnati, Ohio: ACGIH, 2010. pp. 13–134,135.
- Bello, D., Woskie, S.R., Streicher, R. P.: Polyisocyanates in occupational environments: a critical review of exposure limits and metrics. *Am. J. Ind. Med.* 46: 480-91 (2004).
- Bennett, J.S., D.A. Marlow, F. Nourian, J. Breay, A. Feng and M. Methner. Effect of Ventilation Velocity on Hexavalent Chromium and Isocyanate Exposures in Aircraft Paint Spraying. *Journal of Occupational and Environmental Hygiene*. 2018, VOL. 15, NO. 3, 167-181.
- Bennett, J.S., D. Marlow, F. Nourian, et al.: Hexavalent chromium and isocyanate exposures during military aircraft painting under crossflow ventilation. *J. Occup. Environ. Hyg.* 13(5):356-371 (2016).
- Code of Federal Regulations, Part 1910*: “Occupational Safety and Health Standards, Subpart G: Occupational Health and Environmental Control, Standard 1910.94: Ventilation, Section (c)(6): Velocity and airflow requirements.”
- Code of Federal Regulations, Part 1910*: “Occupational Safety and Health Standards, Subpart G: Occupational Health and Environmental Control, Standard 1910.1026: Chromium (IV), part (f)(1)(ii).” Part 1910.
- Lin, C., R. H. Horstman, M. F. Ahlers, L. M. Sedgwick, K. H. Dunn, J. L. Topmiller, J. S. Bennett, S. Wirogo: Numerical Simulation of Airflow and Airborne Pathogen Transport in Aircraft Cabins, Part 2: Numerical Simulation of Airborne Pathogen Transport. *ASHRAE Transactions 2005*, Vol.111, Part I, pp.764-768.
- Patankar, S.V.: *Numerical Heat Transfer and Fluid Flow*. New York: Hemisphere, 1980. pp. 30–39, 126–131.
- U.S. Department of Health and Human Services: *Preventing Asthma and Death from Diisocyanate Exposure*. Centers for Disease Control and Prevention, National Institute for Occupational Safety and Health, DHHS (NIOSH) Publication No. 96-111. 1996.
- U.S. Department of Health and Human Services: *NIOSH ALERT: Preventing asthma and death from MDI exposure during spray-on truck bed liner and related applications*. Centers for Disease Control and Prevention, National Institute for Occupational Safety and Health, DHHS (NIOSH) Publication No. 2006-149. 2006.
- U.S. Department of Health and Human Services: “Workplace Safety and Health Topics: Hexavalent chromium.” Centers for Disease Control and Prevention, National Institute for Occupational Safety and Health. Available at: <http://www.cdc.gov/niosh/topics/hexchrom> (accessed: June 12, 2015).
- U.S. Department of Defense: Unified Facilities Criteria, UFC 4-211-02NF. *Industrial Ventilation*. Ch. 2-4.2.2, Corrosion Control and Paint Finishing Hangars. 2010. p. 12.
- U.S. Department of Health and Human Services: In-depth survey report: experimental and numerical research on the performance of exposure control measures for aircraft painting operations, part II. Centers for Disease Control and Prevention, National Institute for Occupational Safety and Health, EPHB-329-12b, 2012. Available at: www.cdc.gov/niosh/surveyreports/pdfs/329-12b.pdf (accessed 01/03/2017).
- Vandenplas O, Cartier A, Lesage J, et. Al.: Prepolymers of hexamethylene diisocyanate as a cause of occupational asthma. *J. of Allergy and Clin. Immunol.* 91:850-861 (1993).

Reproduced with permission of copyright owner. Further reproduction prohibited without permission.